*Resolving the Rise and Fall of Star Formation in Galaxies*
*Proceedings IAU Symposium No. 373, 2023*
*T. Wong & W.-T. Kim, eds.*
doi:10.1017/S174392132200391X

# Cloud-scale Analyses on Molecular Gas in Simulated and Observed Galaxy Mergers

**Hao He**

McMaster University
1280 Main St W, Hamilton, ON L8S 4L8, CAN

**Abstract.** We employ the Feedback In Realistic Environments (FIRE-2) physics model to study how the properties of giant molecular clouds (GMCs) evolve during galaxy mergers. Due to the rarity of mergers in the local Universe, samples of nearby merging galaxies suitable for studies of individual GMCs are limited. Idealized simulations provide us with a new window to study GMC evolution during a merger, and assist in interpreting observations. We conduct a pixel-by-pixel analysis of the simulated molecular gas properties in both undisturbed control galaxies and galaxy mergers. The simulated GMC-pixels follow a similar trend in a diagram of velocity dispersion ($\sigma_v$) versus gas surface density ($\Sigma_{\rm mol}$) as observed in normal spiral galaxies in the Physics at High Angular resolution in Nearby GalaxieS (PHANGS) survey. For simulated mergers, we see a significant increase in both the $\Sigma_{\rm mol}$ and $\sigma_v$ for GMC-pixels by a factor of 5 – 10, which put these pixels to be above the trend of PHANGS galaxies in the $\sigma_v$ vs $\Sigma_{\rm mol}$ diagram. This deviation indicates that GMCs in the simulated merger are more gravitationally unbound and have higher virial parameter ($\alpha_{\rm vir}$) of 10 – 100, which is much larger than that of simulated control galaxies. Furthermore, we find that the increase in $\alpha_{\rm vir}$ generally happens at the same time as the increase in global star formation rate (SFR), which suggests feedback is playing a role in dispersing the gas. The correspondence between high $\alpha_{\rm vir}$ and SFR also suggests some other physical mechanisms besides self-gravity are helping the GMCs in starburst mergers to collapse and form stars.

**Keywords.** ISM: clouds, ISM: kinematics and dynamics, ISM: structure, galaxies: interactions, galaxies: starburst, galaxies: star formation

## 1. Introduction

Giant molecular clouds (GMCs) are the birth places of stars. Hence, to understand the links between molecular gas and star formation rate (SFR) in galaxies, it is essential to study the physical properties of molecular clouds in a broad range of environments.High-resolution CO observations have successfully characterized GMCs in the Milky Way and nearby galaxies. In particular, the recently completed PHANGS-ALMA survey (Leroy et al. 2021) has expanded these observations across a complete sample of nearby spiral galaxies, providing direct measurements of molecular gas surface density $\Sigma_{\rm mol}$, velocity dispersion $\sigma_v$ and radius $R$, which are key quantities for determining the physical state of GMCs. However, GMCs in galaxy mergers are rarely studied. On the observational side, the scarcity of nearby mergers means that we have only a handful of systems observed with GMC resolution (Brunetti et al. 2021; Brunetti 2022). These studies show that GMCs in mergers have significantly higher gas surface densities and are less gravitationally bound compared to GMCs in normal spirals. However, it is difficult to draw statistically robust conclusions on how GMC properties evolve across various merging stages based on these limited observational samples. Using a comprehensive library of


https://doi.org/10.1017/S174392132200391X Published online by Cambridge University Press

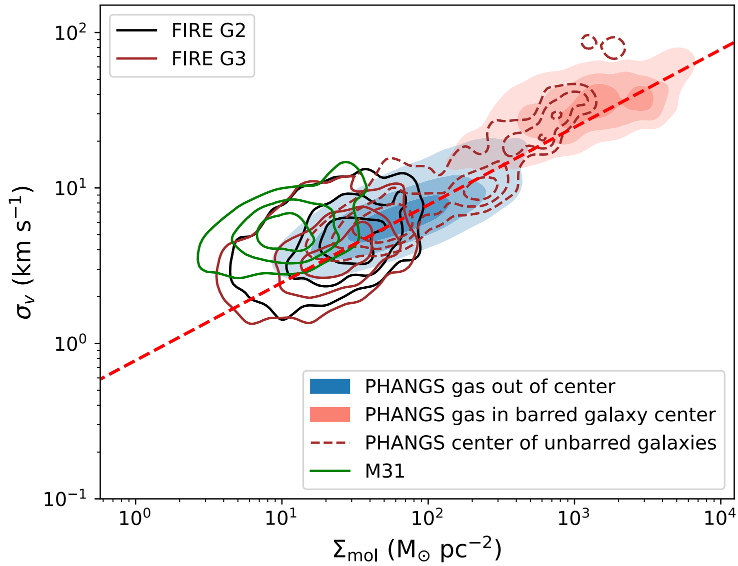


**Figure 1.** Velocity dispersion versus gas surface density for the G2 (black solid line) and G3 (brown solid line) simulated galaxies with inclination angle of 30 degrees compared to the PHANGS galaxy sample. The contour is mass weighted and set to include 20%, 50% and 80% of the data. The density contours of PHANGS galaxies (Sun et al. 2020) show the distribution of measurements in galaxy disks (blue shaded contours), the centers of barred galaxies (Salmon shaded contours) and the centers of unbarred galaxies (brown dashed contours) with a resolution of 90 pc. The red dashed line marks the position with median values of $\alpha_{\rm vir}$ for PHANGS galaxies of 3.1 (Sun et al. 2020). We also show the data for M31 (green solid contour) at 120 pc resolution from Sun et al. (2018). $\Sigma_{\rm mol}$ and $\sigma_v$ for the FIRE-2 spiral galaxies follow a similar trend to the PHANGS galaxies but lie at the lower end of the plot.

idealized galaxy merger simulations based on the FIRE-2 physics model, Moreno et al. (2019) show that SFR enhancement is accompanied by an increase in the cold dense gas reservoir. This suite thus provides us with the ideal tool to properly examine GMC evolution along the entire merging sequence.

## 2. GMCs in the simulated isolated galaxies

To test if the simulation successfully reproduces observed GMCs, Figure 1 shows the well-known correlation between $\sigma_v$ and $\Sigma_{\rm mol}$ for isolated simulated galaxies and PHANGS-ALMA spiral galaxies. The left panel shows $\sigma_v$ versus $\Sigma_{\rm mol}$ contours for G2 and G3 galaxies at an inclination angle of 30 degrees, compared with that of observed galaxies, while the right contour shows the contour for G3 galaxies with different inclination angles. The two simulated galaxies, G2 and G3, exhibit similar properties (black and dark red solid contours) and generally lie on the trend followed by the PHANGS galaxies when viewed at an inclination angle of 30 degrees. We also plot the red dashed line indicating GMCs with constant virial parameter $\alpha_{\rm vir}$ of 3.1. We can see both our simulated galaxies and observed PHANGS galaxies follow the trend of the constant $\alpha_{\rm vir}$, which gives the relation of $\sigma_v^2 \propto \Sigma_{\rm mol}$. For this aspect, the simulations reproduce GMCs similar to the observations. However, we can see that the two galaxies lie at the low surface-density end of the PHANGS distribution and thus their gas properties are more similar to those of M31 than to a typical PHANGS galaxy.

https://doi.org/10.1017/S174392132200391X Published online by Cambridge University Press

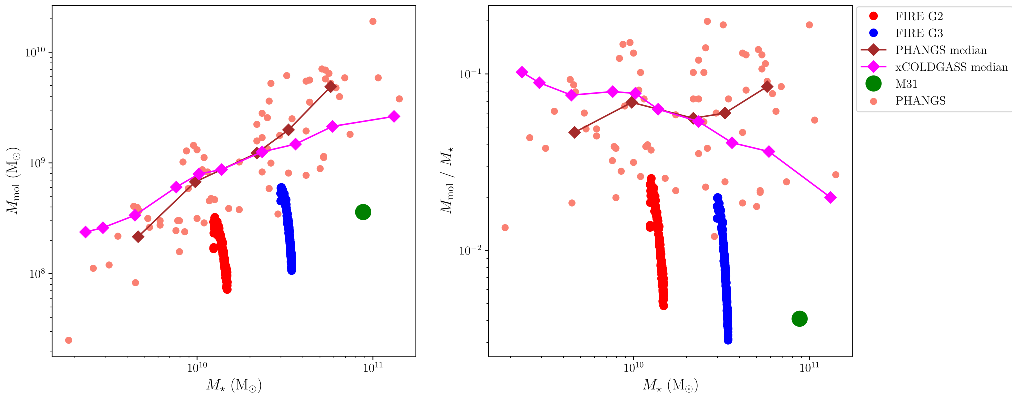


**Figure 2.** (Left) $M_{\rm mol}$ versus $M_\star$ for PHANGS galaxies (salmon dots; Leroy et al. 2021), M 31 (green filled circle, Nieten et al. 2006) and the G2 (red points) and G3 (blue points) simulated galaxies. Note that the G2 and G3 simulated galaxies lie significantly below the star-forming main sequence defined by the xCOLDGASS sample. (Right) $f_{\rm mol}$ versus $M_\star$ for the same galaxies. The molecular gas fractions of G2 and G3 are significantly lower than those of the PHANGS spiral galaxies.

In interpreting the lower $\Sigma_{\rm mol}$ values seen in Fig. 1, one possibility is that there may not be as much gas available to form high surface density clouds in the two simulated galaxies compared to the PHANGS galaxies. Fig. 2 compares the global molecular gas masses, $M_{\rm mol}$, and molecular gas fractions, $f_{\rm mol} = M_{\rm mol} / M_\star$, for the FIRE-2 mergers with those of the PHANGS galaxies from (Sun et al. 2020). We also show the median value of $M_{\rm mol}$ and $f_{\rm gas}$ in each $M_\star$ bin for the PHANGS galaxies, as well as the weighted median of $M_\star$ and $f_{\rm mol}$ for galaxies in xCOLDGASS sample (Saintonge et al. 2017). The two median values are quite close to each other for galaxies with $M_\star$ of $10^{9.5}$ – $10^{11}$ M$_\odot$, although the PHANGS galaxies seem to deviate somewhat from the xCOLDGASS sample in the highest and lowest mass bins. In contrast, the G2 and G3 galaxies both have $f_{\rm mol} \sim 3$ times lower than typical PHANGS or xCOLDGASS galaxies of the same stellar mass. Therefore, the small global $f_{\rm mol}$ may be the cause for producing the low $\Sigma_{\rm mol}$ values seen in the simulated galaxies.

## 3. Merging galaxies

We performed a similar $\sigma_v$ versus $\Sigma_{\rm mol}$ analysis for our suite of galaxy merger simulations. Since we are particularly interested in how the starburst activities influence GMC properties, we focus on the period right before and after then second passage where you can see the largest contrast in SFR. We show the two example snapshots before and after the second passage in Fig. 3. As we can see, the simulated merger still has the similar $\Sigma_{\rm mol}$ and $\sigma_v$ as the isolated galaxies right before the start of the second perihelion passage. Then the molecular gas quickly transitions to a more turbulent state with much higher $\sigma_v$ after the second passage along with dramatic increase in global SFR, as shown in the snapshot at 2.66 Gyr. As shown in the zeroth moment map, the G2&G3 merger at this time still shows two separate nuclei; a similar stage as our observed mergers, the Antennae and NGC 3256. At this time, the $\sigma_v$ versus $\Sigma_{\rm mol}$ contours for the simulated merger lies above the trend seen for the PHANGS galaxies, similar to NGC 3256. In contrast, it is different from the Antennae, which still lies along the trend of PHANGS galaxies. The larger deviation from the PHANGS trend means higher $\alpha_{\rm vir}$.

https://doi.org/10.1017/S174392132200391X Published online by Cambridge University Press

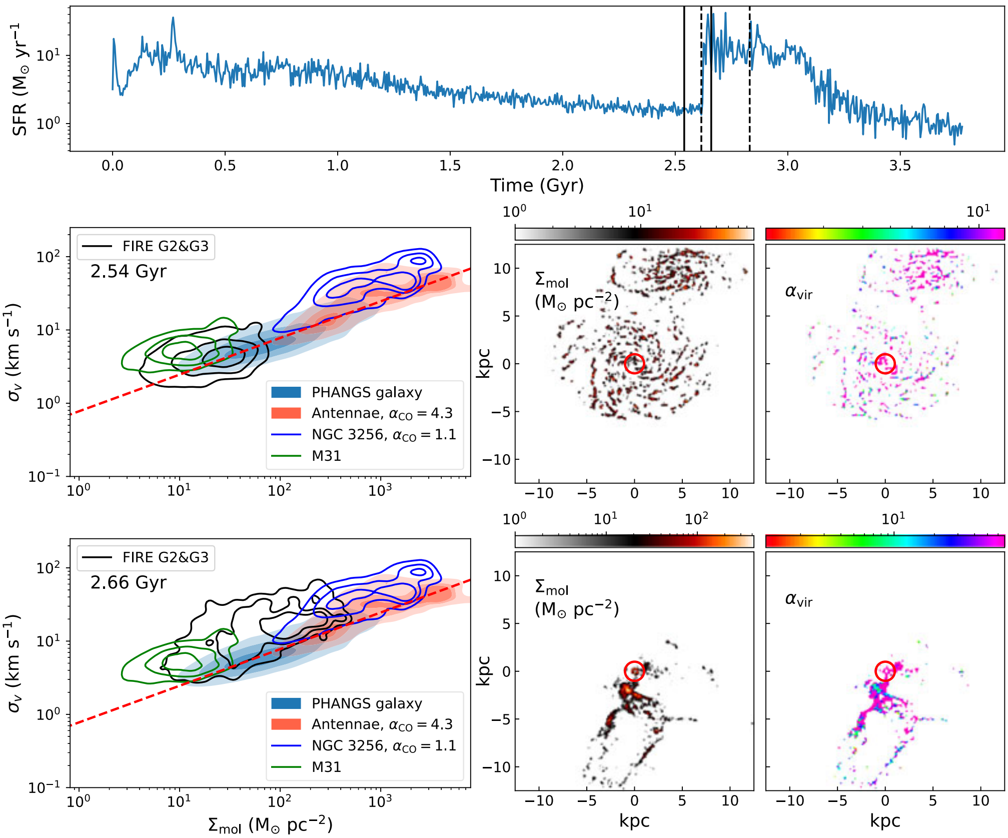


**Figure 3.** Two of the snapshots for the G2&G3 merger with 'e2' orbit with viewing angle of 'v0'. The top panel shows the SFR history for this merging suite. The two solid vertical lines indicate the time for each snapshot. The two dashed lines indicate the times at the start of second merging and the final coalesce of two nuclei. For the bottom snapshots, the left panel shows the $\sigma_v$ versus $\Sigma_{\rm mol}$ mass weighted contour with the same setting as Fig.1. We also show the density contours for the PHANGS galaxies (filled blue region), NGC 3256 (blue contours) and the Antennae (orange shaded region). For NGC 3256, $\Sigma_{\rm mol}$ is calculated using the ULIRG $\alpha_{\rm CO}$ of 1.1 $M_\odot$ (K km s$^{-1}$ pc$^2$)$^{-1}$. For the Antennae, the gas surface density is calculated using the Milky Way $\alpha_{\rm CO}$ of 4.3 $M_\odot$ (K km s$^{-1}$ pc$^2$)$^{-1}$. We also show the $\Sigma_{\rm mol}$ and $\alpha_{\rm vir}$ map for the two snapshots. The interactive version of the animation is available at `https://htmlpreview.github.io/?https://github.com/heh15/merger_animations/blob/main/G2G3_e2_v0.html`.

We note that different $\alpha_{\rm CO}$ choices will affect the position of the contour. If we choose ULIRG $\alpha_{\rm CO}$ instead of the Milky Way value, the Antennae would have $\alpha_{\rm vir}$ similar to that of NGC 3256 and our G2&G3 merger. The uncertainty in the correct $\alpha_{\rm CO}$ value to use makes it difficult to interpret the data for the Antennae in this context. For our further analysis, we will adopt the Milky Way $\alpha_{\rm CO}$ for the Antennae.

### 3.1. *The evolution of virial parameter* $\alpha_{\rm vir}$

During the second passage, we see that the $\sigma_v$ vs $\Sigma_{\rm mol}$ distribution for our simulated mergers lies above the trend observed for the PHANGS galaxies. A higher $\sigma_v$ for a given $\Sigma_{\rm mol}$ means the GMCs in these mergers are more turbulent and less gravitationally bound

https://doi.org/10.1017/S174392132200391X Published online by Cambridge University Press

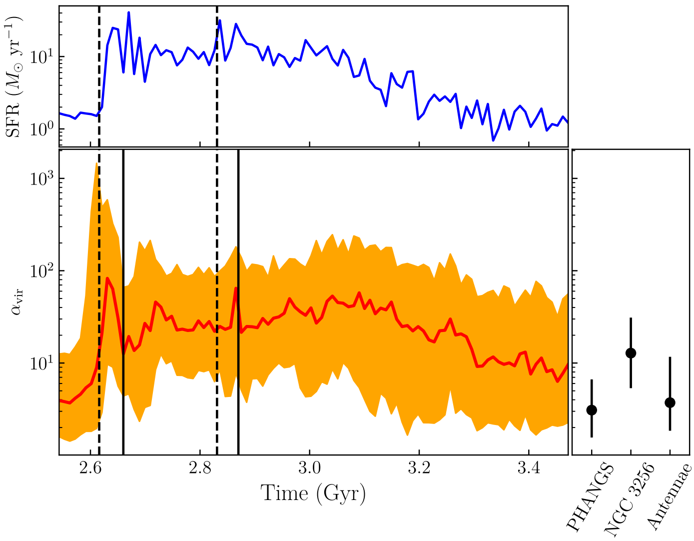


**Figure 4.** The variation of $\alpha_{vir}$ versus time for the G2&G3 mergers in (left) the e2 orbit and (right) the e1 orbit viewed from 'v0' angle during the final coalescence. (**Left**) the red line is the mass weighted median for $\alpha_{vir}$ from the simulation. The orange shaded region includes data within the 16th and 84th quantile of $\alpha_{vir}$ values. The dashed lines correspond to the start of the second passage and the final coalescence of the two nuclei. The two solid lines correspond to the merger times shown in Fig. 3. The upper panel shows SFR vs time for the second coalescence and the right panel shows the 16th, 50th and 84th quantile of $\alpha_{vir}$ for PHANGS, NGC 3256 and the Antennae from the observations. In calculating $\alpha_{vir}$, we use the U/LIRG $\alpha_{CO}$ for NGC 3256 and the Milky Way value for PHANGS and the Antennae. (**Right**) Same plot for G2&G3 merger in the 'e1' orbit during the final coalescence. The 'e1' orbit has a smaller impact parameter than the 'e2' orbit.

than in normal spiral galaxies. We adopt the same approach as in observation to calculate $\alpha_{vir}$ for fixed-scale GMC pixels as (Sun et al. 2018)

$$\begin{aligned}\alpha_{vir} &= \frac{9\ln 2}{2\pi G}\frac{\sigma_v^2}{\Sigma_{mol}R} \\ &= 5.77\left(\frac{\sigma_v}{\text{km } s^{-1}}\right)^2\left(\frac{\Sigma_{mol}}{\text{M}_\odot}\right)^{-1}\left(\frac{R}{40\text{ pc}}\right)^{-1} \end{aligned} \tag{1}$$

where $R$ is the radius of GMCs. In Sun et al. (2018), $R$ is set to be the radius of the beam in the image, as each beam is treated as an independent GMC. For the simulation data, we do not have a telecope beam to convolve with, so we set $R$ to be half the size of each pixel as each pixel can be treated as an independent GMC. We note that the pixel in simulation is equivalent to the beam in observation since both are independent measurement units. With $R$ a constant, $\alpha_{vir}$ depends only on $\sigma_v$ and $\Sigma_{mol}$. The higher $\sigma_v$ at a similar $\Sigma_{mol}$ thus implies that $\alpha_{vir}$ values for GMCs in simulated mergers are higher than the values for PHANGS or simulated isolated galaxies. Higher values for $\alpha_{vir}$ are also found for NGC 3256 (Brunetti et al. 2021) and the Antennae (Brunetti 2022). Fig. 4 shows $\alpha_{vir}$ as a function of time during the period near the second pericentric passage for the merger simulation with "e2" and "e1" orbit and viewed from "v0" angle. We can see that $\alpha_{vir}$ stays low before the second passage and suddenly rises after the passage along with a sudden increase in SFR. The peak of median $\alpha_{vir}$ can reach $\sim 100$. We note that both the Antennae and NGC 3256 are at the very start of their second passages. In this stage, $\alpha_{vir}$ is quite time-sensitive and it is hard to match the exact same stage

https://doi.org/10.1017/S174392132200391X Published online by Cambridge University Press

between the simulated and observed galaxies. Therefore, it is possible that both NGC 3256 and Antennae are caught at a specific merger stage with a lower $\alpha_{\rm vir}$ (although in the case of NGC 3256, still enhanced relative to PHANGS galaxies). In comparison, $\alpha_{\rm vir}$ in the simulations is relatively stable in the post merger stage. This stability suggests that a comparison between simulations and observations of post merger galaxies could be a useful next step. In addition, post mergers have rather simple morphology, which simplifies the task of making quantitative comparisons.

## 4. Future work

In the future, we would like to expand our comparison to more observed and simulated mergers. From the observational side, we need larger samples of galaxy mergers spanning different evolutionary stages in order to understand how GMCs evolve throughout the merging. In addition, it is easier to compare the observations with simulations at post-merger stages since the morphology is simpler and easier to quantify. In the ALMA archive, we have already had at least 10 U/LIRGs with GMC resolution CO 2-1 observations. We can utilize these archival data to build a more complete sample of GMCs in mergers at different stages. From the simulation side, we can see that the initial set-up could affect our interpretation on the simulation results. Therefore, it is necessary for us to compare with simulations that better match the observed galaxies. For the two observed mergers we have, the Antennae has been widely studied and matched by non-cosmological simulations (e.g. Renaud et al. 2019a; Li et al. 2022). Besides comparing with these non-cosmological simulations, we could also compare observation with some latest cosmological simulations, such as FIREBox (Feldmann et al. 2022), that includes local mergers.

### References

Brunetti, N., Wilson, C.D., Sliwa, K. 2021, MNRAS, 500, 4730
Brunetti, N. 2022, thesis
Feldmann, R., Quataert, E., Faucher-Gigu‘ere, C.-A., et al. 2022, 2022arXiv220515325F
Leroy, A. K., Hughes, A., Schruba, A., et al. 2016, ApJ, 831, 16
Leroy, A. K., Schinnerer, E., Hughes, A., et al. 2021, ApJS, 257, 43
Li, H., Vogelsberger, M., Bryan, G. L., et al. 2022, MNRAS, 514, 265
Moreno, J., Torrey, P. Ellison, S., 2019, MNRAS, 485, 1320
Nieten, C., Neininger, N., Gu'elin, M., et al. 2006, A&A, 453, 459
Renaud, F., Bournaud, F., Agertz, O., et al. 2019a, A&A, 625, A65
Saintonge, A., Catinella, B., Tacconi, L. J., et al. 2017, APJS, 233, 220
Sun, J., Leroy, A. K., Schruba, A., et al. 2018, ApJ, 860, 172
Sun, J., Leroy, A. K., Schinnerer, E., et al. 2020, ApJL, 901, L8